

Thermoelectric properties of CoSb₃ and related alloys

J. W. Sharp,^{a)} E. C. Jones,^{a)} R. K. Williams,^{b)} P. M. Martin,^{b)} and B. C. Sales^{c)}
Oak Ridge National Laboratory, Oak Ridge, Tennessee 37831-6056

(Received 30 January 1995; accepted for publication 6 April 1995)

Seebeck, electrical, and thermal conductivity data are reported on CoSb₃, and doped and undoped alloys of Co_{1-x}Ir_xSb_{3-y}As_y from 20 to 700 K. *n*-type semiconductors were obtained by doping with Ni, Te, or Pd, and the hole concentration in *p*-type samples was increased by substitution of Fe, Ru, Os, and Ge. An estimated maximum value for ZT of 0.6 (*Z* is the figure of merit) was found for a Te-doped (*n*-type) alloy at 700 K. For *p*-type alloys, the maximum value of ZT was found to be 0.3 at 550 K. Electrical and thermal transport data also are reported for CoAs₃, RhSb₃, and IrSb₃. Most of the samples investigated were polycrystalline, but a few measurements on CoSb₃ single crystals also are discussed. © 1995 American Institute of Physics.

I. INTRODUCTION

Good thermoelectric materials combine a large Seebeck coefficient (*S*) with low electrical resistivity (ρ) and low thermal conductivity (κ). This requirement follows from the dependence of thermoelectric device performance on the operating temperatures and the figure of merit, $Z = S^2/\rho\kappa$: for power generation,

$$\text{Efficiency} = \frac{(T_h - T_c)(\gamma - 1)}{T_c + \gamma T_h}$$

and for refrigeration,

$$\text{Coefficient of Performance} = \frac{\gamma T_c - T_h}{(T_h - T_c)(1 + \gamma)}, \quad (1)$$

where T_c (T_h) is the temperature of the cold (hot end), and $\gamma = \sqrt{1 + ZT}$ varies with the average temperature, $T = (T_c + T_h)/2$.¹ For both applications, effectiveness increases monotonically with ZT, and ZT=1 is a viability benchmark.

Not all materials need to be considered as potential thermoelectrics. For ordinary metals the Seebeck coefficient is too low. For intrinsic semiconductors the ratio of the electrical to thermal conductivity is too low.² Consequently, the best thermoelectrics discovered are semiconductors that have been doped and alloyed to maximize *Z*.³ Si_{0.8}Ge_{0.2} is favored for power generation at high temperatures, and solutions of (Sb,Bi)₂(Se,Te)₃ are used in thermoelectric refrigerators.³ In both cases, ZT \leq 1 at the operating temperature. As part of an ongoing search for better thermoelectric refrigeration materials, we have conducted a reasonably thorough investigation of the semiconductors CoSb₃, CoAs₃, IrSb₃, and associated alloys. These compounds were considered good candidates because they are covalently bonded, perhaps yielding high carrier mobilities, and they have a large number of atoms per unit cell, a trait associated with low lattice thermal conductivity.⁴ Our results for IrSb₃ are much less promising than those reported very recently by others.⁴ Many of the conclusions of prior examinations^{5,6} of the transport proper-

ties of CoSb₃ and CoAs₃ have been confirmed and extended by this work. Briefly, these materials fail as thermoelectric materials because they exhibit modest carrier mobilities but efficient heat transport by the lattice. The crystal structure of all of these compounds has 32 atoms per unit cell, but the low metalloid coordination number (4) may be responsible for the large lattice thermal conductivity.⁷ In the present work the best material achieved, Co_{0.97}Ir_{0.03}Sb_{2.81}Te_{0.04}As_{0.15}, has ZT \approx 0.6 at *T*=700 K.

The semiconductors (Co,Rh,Ir)(P,As,Sb)₃ crystallize in the skutterudite structure.⁸ This structure is cubic with 32 atoms per unit cell (space group *Im*3). Each metal atom has six metalloid neighbors octahedrally arranged. Each metalloid atom has two metalloid and two metal neighbors, the four forming a tetrahedral arrangement. Alternately, the skutterudite structure can be described as consisting of square planar rings of four metalloid atoms with the rings oriented along either the (100), (010), or (001) crystallographic directions. The metal atoms form a simple cubic sublattice with a subcell dimension of *a*/2. Optical measurements give the band gaps of IrSb₃ and CoAs₃ as 1.4 and 0.2 eV, respectively.^{9,10} Electrical resistivity data (see below) indicate a conduction band gap (E_g) of 0.6–0.7 eV for CoSb₃, in agreement with recent estimates from band structure calculations.¹¹ Because intrinsic conduction is negligible for $E_g > 10k_B T$, these materials can be doped for optimal thermoelectric performance at and below room temperature. The extrinsic carrier type depends on the number of valence electrons of the dopant atom in the usual manner: The hole concentration was increased by addition of Fe, Ru, Os, and Ge, and *n*-type samples were achieved by doping with Ni, Pd, and Te.

II. EXPERIMENT

As discussed later, ZT for a CoSb₃ single crystal was estimated to be nearly the same as for polycrystalline CoSb₃. Because single crystals are more difficult to obtain, the thermoelectric properties of the skutterudites were gleaned by studying a large number of polycrystalline samples. Stoichiometric mixtures of Sb (99.9999%), Co (99.998%), and Ir (99.99 or 99.95%) powders were ground together in air and heated in evacuated fused silica ampoules at 600–700 °C for

^{a)}Solid State Division.

^{b)}Metals and Ceramic Division.

^{c)}Author to whom correspondence should be addressed.

two to three days. Arsenic chunks (99.9999%) were added in a helium drybox, and the stoppered ampoule was evacuated without significant air exposure. Following powder reaction, 3/4-in.-diam pellets were formed by hot pressing (10^7 Pa, 600–700 °C), or cold pressing (10^7 Pa) and sintering at 700 °C, for the triantimonides and 600 °C for the triarsenide. For CoAs_3 and the alloys, only cold-pressed samples were made. During hot-pressing the triantimonide pellets were enveloped by graphite foil. For sintering, cold-pressed pellets were placed in an alumina (99.9%) crucible that rested in an evacuated fused silica tube. Except for alloyed samples, only the skutterudite phase was observed in powder x-ray diffraction patterns. All samples exhibited long-term stability in air. The respective densities of hot and cold-pressed samples were nominally 90% and 70% of the ideal (*x*-ray) densities for the triantimonides. CoAs_3 pellets had a density of only $\sim 50\%$ of the ideal value. Hot-pressed samples handled well for cutting and sanding, but cold-pressed samples were susceptible to cracking. Dopants usually were added between powder reaction and pressing, although occasionally the dopant was included in the powder reaction. The lightest dopant concentrations were obtained by dilution of more heavily doped pellets.

The alloying behavior of these compounds is noteworthy. At 650 °C, midway between the usual processing temperatures for CoSb_3 and CoAs_3 , pellets containing 25% and 50% CoAs_3 decomposed badly. After cooling, the result was a deposit of an Sb-As alloy and a pellet that had significant amounts of both $\text{CoSb}_{3-x}\text{As}_x$ and $\text{CoSb}_{2-y}\text{As}_y$. Only a small amount of decomposition occurred in a 12% CoAs_3 sample sintered at 700 °C. At 550 and 600 °C, CoSb_3 and CoAs_3 did not alloy during 50–100 h anneals. It was found that bismuth does not substitute for antimony in CoSb_3 , in agreement with the previous study.⁵

For Seebeck coefficient, four-point electrical resistivity, and van der Pauw configuration Hall probe measurements, rectangular slabs ($\sim 0.15 \times 0.5 \times 1.8$ cm³) were cut from the fired pellets. The slabs were sanded just prior to mounting in the measurement systems to avoid artifacts associated with surface layers, though we have seen no evidence that this is a substantial problem with these compounds. Electrical resistance and thermopower measurements were made from 20 to 300 K in an automated closed-cycle refrigeration system, and from 300 to 700 K in an automated furnace system. A standard technique¹² was employed, with a small heater to establish a temperature gradient, two 5 mil type E thermocouples for temperature measurements, and two 3 mil Cu wires as voltage leads. Each thermocouple and the corresponding voltage lead were electrically and thermally sunk to the sample using silver paint. To facilitate current flow for resistance measurements, the sample was bonded to metal endplates with silver paint. Occasional testing against Pt and constantan standards indicated errors of $\pm 5\%$ for both *S* and ρ values, with most of the error in ρ resulting from estimation of the length of the sample between the voltage contacts. The *S* values presented here are relative to Cu, a close approximation to the absolute thermopower for a good thermoelectric. Carrier concentrations at 300 and 77 K that were less than $\sim 2 \times 10^{19}$ cm⁻³ were determined within $\pm 20\%$ us-

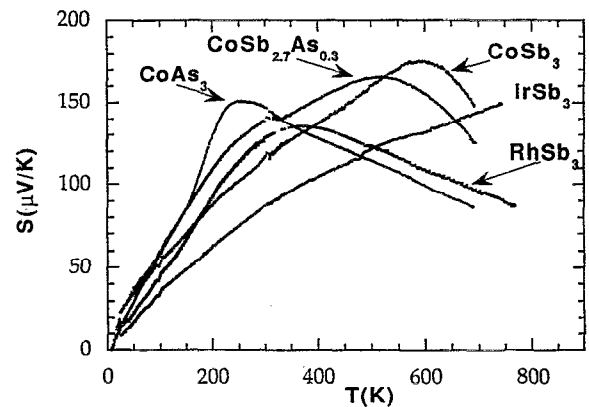


FIG. 1. Thermopower versus temperature for several undoped skutterudite compounds and alloys. RhSb_3 was a hot-pressed ceramic with 94% of the theoretical *x*-ray density (7.9 g/cm³). The remaining materials were cold-pressed and sintered and, with the exception of CoAs_3 , had densities about 70% of the theoretical maximum. The density of the soft CoAs_3 ceramic was only about 47% of maximum.

ing a Hall effect system with a 0.5 T magnet. Additionally, for hot-pressed samples more accurate measurements of carrier concentrations were made from 325 to 4.2 K using an 8 T Hall effect system. Thermal conductivity measurements were made in the range 300–370 K on 1/4-in.-diam disks machined from larger hot-pressed pellets, and on 1/4-in.-diam cold-pressed, sintered pellets. To obtain the thermal conductivity accurately, account must be taken of heat transfer by processes other than conduction within the solid.¹² In the apparatus used here, several type E thermocouples profile the temperature along two Armco iron rods that sandwich the sample, with indium coupling at the contacts. Errors of less than $\pm 3\%$ are achieved by this technique.¹³

III. RESULTS AND DISCUSSION

Thermopower and resistivity data for the undoped, cold-pressed skutterudites are presented in Figs. 1 and 2. Synthesis by cold pressing yielded *p*-type materials with carrier

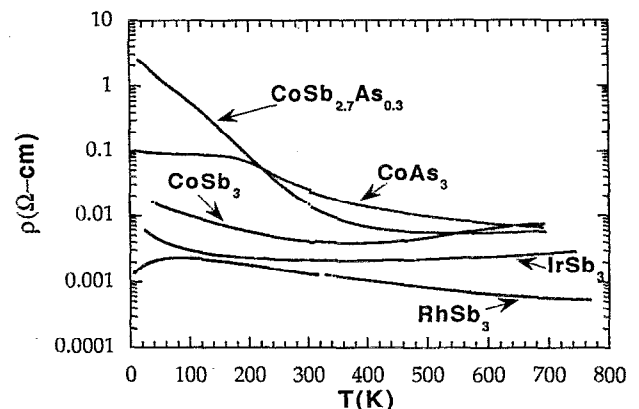


FIG. 2. Resistivity vs temperature for several undoped skutterudite compounds and alloys. The thermopower data for these same samples are shown in Fig. 1.

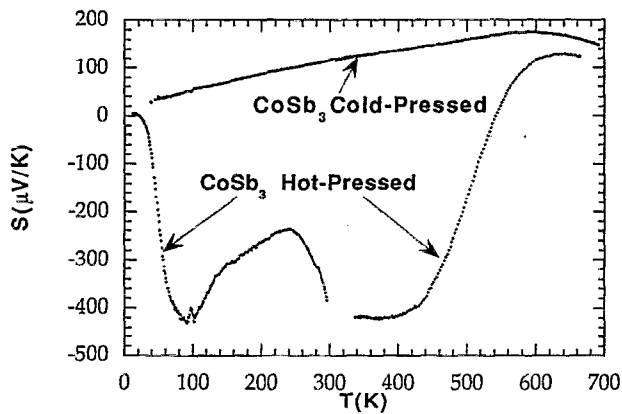


FIG. 3. Thermopower vs temperature for hot-pressed and cold-pressed CoSb_3 . It is likely that during the hot-pressing of this compound enough Sb is lost to change the material from p type to n type. The peak at 100 K for the n -type material is probably due to phonon drag.

concentrations of 0.8, 2–5, and $3\text{--}10 \times 10^{18} \text{ cm}^{-3}$ for CoAs_3 , CoSb_3 , and IrSb_3 , respectively, at room temperature. Higher carrier concentrations were found for IrSb_3 that were synthesized using an Ir source that contributed approximately $5 \times 10^{18} \text{ cm}^{-3}$ acceptors. The resistivities increase at low temperatures primarily because the mobilities decrease, with only slight decreases in carrier concentrations. This result suggests that below room temperature the holes predominantly scatter from ionized defect levels that are slightly above the valence band edge. At higher temperatures the resistivity of CoAs_3 decreases due to activation of intrinsic carriers across the band gap.¹⁰ For the other materials, (except RhSb_3) the resistivity rises at higher temperatures, suggesting that hole mobility is limited by electron-phonon scattering. The RhSb_3 data shown in Figs. 1 and 2 are from a hot-pressed sample. This material was p -type with a hole mobility of about $1000 \text{ cm}^2/\text{Vs}$ and a carrier concentration of $1 \times 10^{19} \text{ cm}^{-3}$.

The Seebeck coefficients of the skutterudites increase linearly or sub-linearly with temperature until intrinsic conduction becomes active, at which point there is a peak fol-

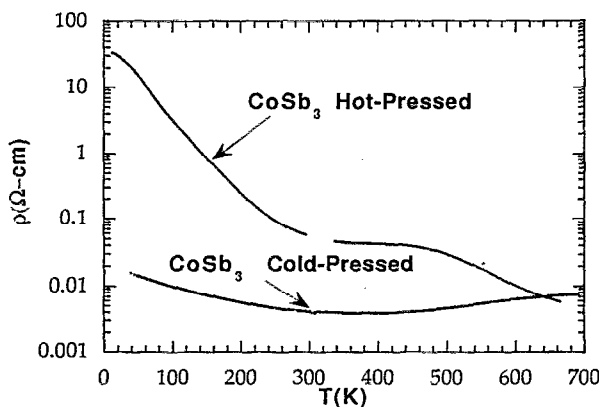


FIG. 4. Resistivity vs temperature for hot-pressed and cold-pressed CoSb_3 . The thermopower data for these samples are shown in Fig. 3.

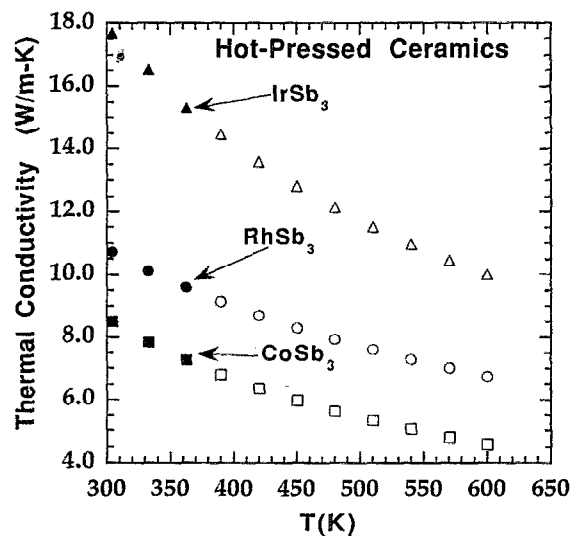


FIG. 5. Total thermal conductivity versus temperature for hot-pressed skutterudite ceramics. The ceramics had densities that were typically 92%–95% of the theoretical x-ray density. The solid points are the experimental data, while the open points represent an extrapolation of the data to higher temperatures.

lowed by a decline. A qualitative understanding of thermopower data is most easily achieved by noting that S is the average energy per carrier (measured from the Fermi energy) divided by the electronic charge and the absolute temperature.¹⁴ Below the thermopower peak, the increase with temperature is consistent with a picture in which a growing fraction of holes in a narrow defect band transport an energy slightly greater than $k_B T$. For IrSb_3 no Seebeck peak is observed because conduction by intrinsic carriers is negligible.

Transport properties of hot-pressed and cold-pressed CoSb_3 samples are compared in Figs. 3 and 4. For undoped materials, hot-pressing of CoSb_3 was the only combination

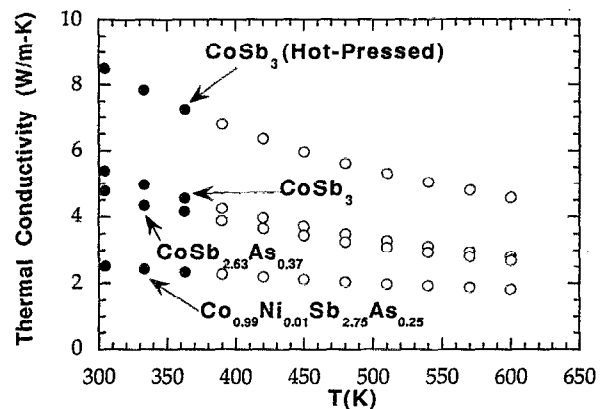


FIG. 6. Total thermal conductivity vs temperature for hot-pressed CoSb_3 and for cold-pressed CoSb_3 and related alloys. The density of the hot-pressed sample was 92% of the theoretical x-ray density, and the density of the cold-pressed ceramics was typically 70% of the maximum. The solid points are the experimental data, while the open points represent an extrapolation of the data to higher temperatures.

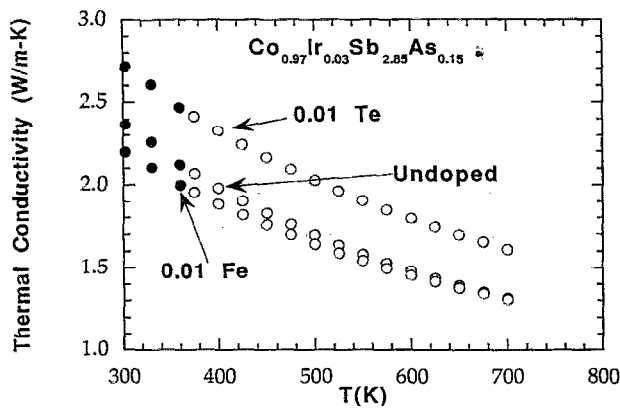


FIG. 7. Total thermal conductivity vs temperature for doped and undoped cold-pressed alloys of $\text{Co}_{0.97}\text{Ir}_{0.03}\text{Sb}_{2.85}\text{As}_{0.15}$. The solid points are the experimental data, while the open points represent an extrapolation of the data to higher temperatures.

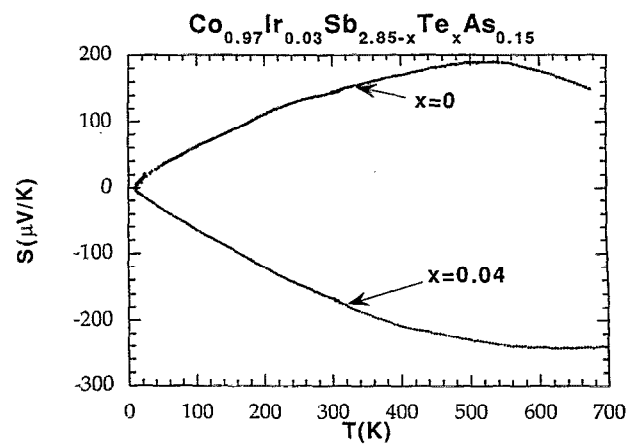


FIG. 8. Thermopower vs temperature for the p - and n -doped alloys of $\text{Co}_{0.97}\text{Ir}_{0.03}\text{Sb}_{2.85}\text{As}_{0.15}$ with the highest value of ZT .

of material and processing step that generated n -type ($\sim 2 \times 10^{18} \text{ cm}^{-3}$) conduction, which has been attributed to a slight Sb deficiency.⁵ Loss of antimony during hot pressing is possible. For hot-pressed CoSb_3 , a conductivity band gap of 0.6–0.7 eV was obtained by fitting the temperature dependent total carrier concentration¹⁵ (extrinsic plus intrinsic) to the resistivity data for $T > 400$ K. The optimum band gap varies slightly depending on whether the mobility is assumed to vary as $T^{-3/2}$ or is held constant.

Thermal conductivity data for 300–370 K are contained in Figs. 5–7, along with estimates obtained by extrapolation to higher temperatures. Thermal conductivity data for hot-pressed samples of IrSb_3 , RhSb_3 , and CoSb_3 are shown in Fig. 5. These data do not follow the rule that larger formula mass leads to lower thermal conductivity, probably because the melting points of these skutterudites increase with formula mass. Data for hot-pressed and cold-pressed CoSb_3 (Fig. 6) verify that the thermal conductivity scales with the density. Substitution of As for 8% of the Sb (or Ir for Co) in CoSb_3 shortens the phonon mean free path and decreases the thermal conductivity. Unfortunately, if more As is incorporated decomposition occurs during processing, and the thermal conductivity increases rather than decreasing further. Because As and Ir enter as neutral atoms in the lattice, they have little effect on the thermopower or electrical resistivity,

and the figure of merit is increased by alloying. Figure 7 contains thermal conductivity data for doped and undoped samples of the alloy $\text{Co}_{0.97}\text{Ir}_{0.03}\text{Sb}_{2.85}\text{As}_{0.15}$ that possessed the highest ZT . Most of the variation in the room temperature thermal conductivities of these alloys (Fig. 7) is due to differences in density and microstructure that occur during processing. Based on the measured electrical conductivity (Table I) it is estimated that the electronic contribution to the thermal conductivity is 5%–15% of the total, an unfavorable condition for thermoelectric applications.

In order to estimate Z at $T > 370$ K, the thermal conductivity results were extrapolated by fitting

$$\kappa = (a + bT)^{-1} \quad (2)$$

to the data. Equation (2) is an often used approximation of the temperature dependence of the phonon conductivity. As a check of the validity of these extrapolations, we estimate $\kappa = 10$ W/m K for hot-pressed IrSb_3 at 600 K, compared with a measured value of 8.5 W/m K given in the literature.⁹

For a semiconductor with a band gap much greater than $k_B T$, a dramatic increase in Z can be achieved by doping because the electrical resistivity decreases sharply with only a modest decrease in S . Figures 8 and 9 display thermopower and resistivity data for the doped alloys with the highest Z . The best p -type and n -type samples result from the as-

TABLE I. Transport properties of some cold-pressed skutterudites at room temperature.

Compound	Carrier density (10^{18} cm^{-3})	Mobility ($\text{cm}^2/\text{V s}$)	Resistivity ($\text{m}\Omega \text{ cm}$)	Seebeck coefficient ($\mu\text{V}/\text{K}$)	Thermal conductivity ($\text{W}/\text{m K}$)	ZT
CoSb_3	5.0	310	4.0	+120	5.3	0.02
CoAs_3	0.8	320	24	+145	...	
IrSb_3	10	460	1.3	+80	12	0.01
$\text{CoSb}_{2.7}\text{As}_{0.3}$	3.7	120	14	+140	...	
$\text{Co}_{0.97}\text{Ir}_{0.03}\text{Sb}_{2.85}\text{As}_{0.15}$						
n type	40	40	3.9	-165	2.4	0.09
p type	3.9	240	5.2	+145	2.4	0.05

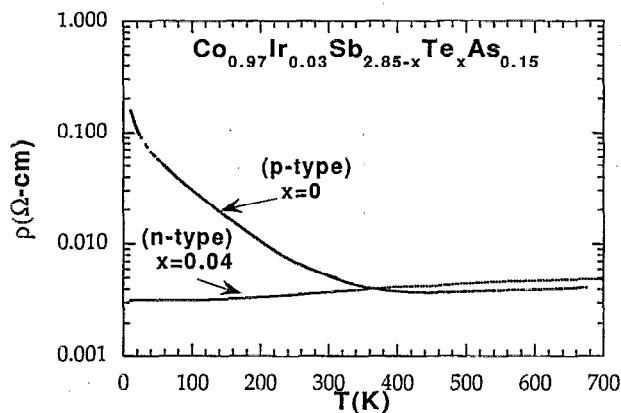


FIG. 9. Resistivity vs temperature for the *p*-doped and *n*-doped alloys of $\text{Co}_{0.97}\text{Ir}_{0.03}\text{Sb}_{2.85-x}\text{Te}_x\text{As}_{0.15}$ with the highest value of *ZT*. The increase of ρ below room temperature for the *p*-type specimen is partially due to carrier freeze-out, indicating a slight activation energy.

prepared alloy ($\text{Co}_{0.97}\text{Ir}_{0.03}\text{Sb}_{2.85}\text{As}_{0.15}$) and from an alloy doped with Te ($\text{Co}_{0.97}\text{Ir}_{0.03}\text{Sb}_{2.81}\text{Te}_{0.04}\text{As}_{0.15}$). At concentrations less than 0.01–0.02, both Fe and Te behave as electrically active dopants, and the carrier concentration increases linearly with impurity concentration. Data taken on cold-pressed $\text{Co}_{1-x}\text{Fe}_x\text{Sb}_3$ samples (not shown) indicated that the optimum iron doping occurred for $x=0.002$. Comparing these data with the data from the undoped (i.e., unintentionally doped) $\text{Co}_{0.97}\text{Ir}_{0.03}\text{Sb}_{2.85}\text{As}_{0.15}$ alloy indicated that this autodoped alloy has a carrier concentration close to optimal. Other dopants were also investigated. It was found that nickel is only slightly inferior to Te for making *n*-type samples. As an acceptor, tin is believed to yield considerably lower *Z* values than Fe.⁵ For optimally doped samples, the carrier concentration and mobility are usually the same at 300 and 77 K, suggesting that the Fermi energy is almost coincident with the extended band edge. The resistivity increases slowly with temperature above 300 K due to increased scattering by phonons.

The product *ZT* is given for the best *p*-type and *n*-type samples in Figs. 10 and 11. Five percent errors in both *S* and ρ lead to a $\pm 15\%$ error in *ZT*. Unfortunately, the error in the extrapolated κ values is unknown. Near 500 K both the *n*- and *p*-type samples have *ZT* values of about 0.3. A report⁴ that *ZT* exceeds 1.5 for IrSb_3 around 500 K was based on faulty measurements, while the less favorable values of *S*, ρ , and κ presented here are in close agreement with those of others.⁹ Although *ZT* is at 0.6 and is rising for the *n*-type sample at 700 K, CoSb_3 based alloys are not stable at significantly higher temperatures. Therefore, $\text{Bi}_2\text{Te}_{2.25}\text{Se}_{0.75}$, which has *ZT*=0.9 at 500 K, still appears to be the most efficient *n*-type material in this temperature range.³

It was thought that larger *Z* values might be obtained for single crystal CoSb_3 samples, and attempts were made to fabricate these by flux growth and by the Bridgeman technique. In both cases there were larger Sb inclusions, but it was possible to extract measurable slabs of CoSb_3 from the Bridgeman-grown crystal. For two samples of this crystal, the thermopower ($60 \mu\text{V/K}$) and resistivity ($0.4 \text{ m}\Omega \text{ cm}$) at

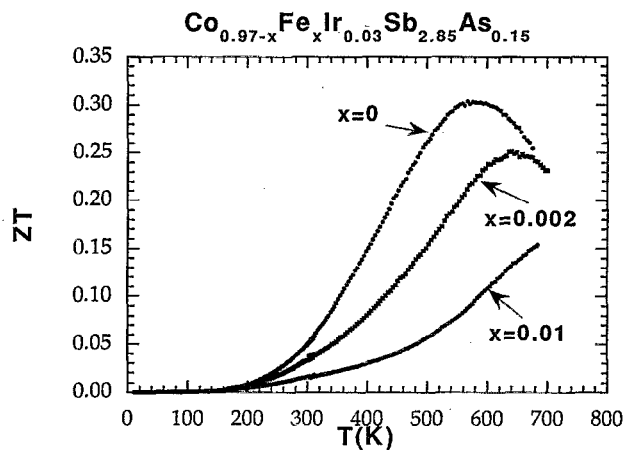


FIG. 10. *ZT* vs temperature for the best *p*-type alloys of $\text{Co}_{0.97-x}\text{Fe}_x\text{Ir}_{0.03}\text{Sb}_{2.85}\text{As}_{0.15}$. The thermal conductivity data from 300 to 370 K were extrapolated to higher (and lower) temperatures.

300 K indicate a processing-induced carrier concentration in the low 10^{19} cm^{-3} range. Assuming that its thermal conductivity is greater than that of cold-pressed CoSb_3 by the appropriate mass density factor, the *ZT* of the crystal is perhaps 10% better than that of low-density polycrystalline material.

Transport data at room temperature for some of the cold-pressed and sintered ceramic compounds and alloys are summarized in Table I. The typical mobilities for *p*-type and *n*-type ceramics were 200–500 $\text{cm}^2/\text{V s}$ and 20–80 $\text{cm}^2/\text{V s}$, respectively. From these data and the data shown in the preceding figures, it seems unlikely that a superior thermoelectric material will be found in the skutterudite family.

ACKNOWLEDGMENTS

This research was supported in part by a Cooperative Research and Development Agreement, Contract No. ORNL92-0116, in part by the Oak Ridge Institute for Science Education, and in part by the Division of Materials

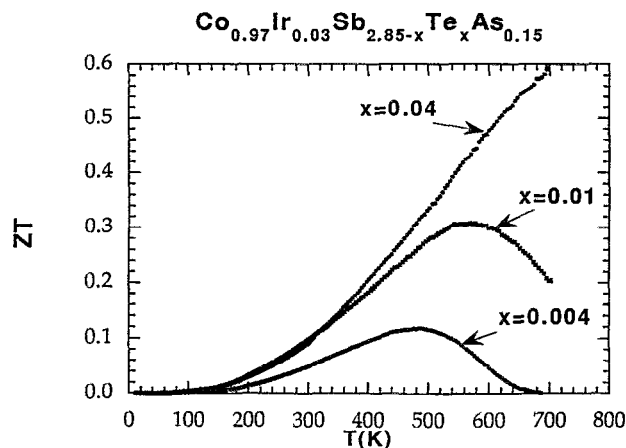


FIG. 11. *ZT* vs temperature for the best *n*-type alloys of $\text{Co}_{0.97}\text{Ir}_{0.03}\text{Sb}_{2.85-x}\text{Te}_x\text{As}_{0.15}$. The thermal conductivity data from 300 to 370 K were extrapolated to higher (and lower) temperatures.

Sciences, U. S. Department of Energy under Contract No. DE-AC05-84OR21400 with Martin Marietta Energy Systems, Inc. The authors take pleasure in thanking J. O. Sofo, G. D. Mahan, H. B. Lyon, T. Caillat, and J. P. Fleurial for informative discussions.

¹R. R. Heikes and R. W. Ure, Jr., in *Thermoelectricity: Science and Engineering*, edited by R. R. Heikes and R. W. Ure, Jr. (Interscience, New York, 1961), Chap. 1, pp. 1–6; R. W. Ure, Jr. and R. R. Heikes, *ibid.* Chap. 15, pp. 458–517.

²J. R. Drabble and H. J. Goldsmid, in *Thermal Conduction in Semiconductors* (Pergamon, New York, 1961), p. 199.

³C. Wood, *Rep. Prog. Phys.* **51**, 459 (1988).

⁴T. Caillat, A. Borshchevsky, and J.-P. Fleurial, in *Proceedings of the XIIth International Conference on Thermoelectrics*, edited by K. Matsuura, Yokohama, Japan, Nov. 9–11, 1993 (1994).

⁵L. D. Dudkin and N. Kh. Abrikosov, *Sov. Phys. Solid State* **1**, 126 (1959).

⁶C. M. Pleass and R. D. Heyding, *Can. J. Chem.* **40**, 590 (1962).

⁷D. P. Spitzer, *J. Phys. Chem. Solids* **31**, 19 (1970).

⁸J. Ackerman and A. Wold, *J. Phys. Chem. Solids* **38**, 1013 (1977).

⁹G. A. Slack and V. G. Tsoukala, *J. Appl. Phys.* **76**, 1665 (1994).

¹⁰G. Kliche and W. Bauhofer, *J. Phys. Chem. Solids* **49**, 267 (1988).

¹¹D. J. Singh and W. E. Pickett, *Phys. Rev. B* **50**, 11235 (1994).

¹²J. E. Bauerle, P. H. Sutter, and R. W. Ure, Jr., in *Thermoelectricity: Science and Engineering*, edited by R. R. Heikes and R. W. Ure, Jr. (Interscience, New York, 1961), Chap. 10, pp. 285–338.

¹³R. K. Williams, R. K. Nanstad, R. S. Graves, and R. G. Berggren, *J. Nucl. Mater.* **115**, 211 (1985).

¹⁴P. M. Chaikin, in *Organic Superconductivity*, edited by V. Z. Kresin and W. A. Little (Plenum, New York, 1990), pp. 101–115.

¹⁵S. M. Sze, *Semiconductor Devices: Physics and Technology* (Wiley, New York, 1985), p. 26.